Research on Vibration Signals of Gearbox in Wind Turbines Under Different Load With Hilbert Huang Transform Method

Han Qingpeng*, Li Tiancheng, Zhu Rui, Li Chenchen

College of Energy and Mechanical Engineering, Shanghai University of Electric Power, Shanghai 200090, China

Abstract: Gearbox and the inside geared rotor systems are core parts in wind turbine which can realize the transmission and energy transfer from wind blades to electric generator. The vibration properties of the gearbox together with its geared rotor systems under sever loading prominently determine the efficiency and operating quality, even the whole life expectation and reliability of the wind turbine. Here, the vibration behaviors are predicted and analyzed for the gearbox and the geared rotor systems of popularly used wind turbines. Experimental measurements of vibrations on the wind turbine gearbox under severe loading are performed on the test-rig and on-site. The vibration signals of different testing points are analyzed in time and frequency domains to explore the underlying complicated behaviors. Hilbert-Huang transform (HHT) method is applied in this paper to distinguish the difference load of vibration signals. Firstly, Hilbert-Huang transform is briefly introduced. Secondly, vibration signals of different load are described by Empirical Mode Decomposition (EMD) and Hilbert spectra. With these results, the vibration signals are distinctly different from each other. It is proved that different load can bring differnt vibration effect of the gearbox through the above comparisons. In sum, the technologies and results of this work provide some good references for vibration prediction and analysis for gearbox and its geared rotor system of wind turbine.

Keywords: Vibration signals, Gearbox, Wind turbines, Hilbert Huang Transform Method, Vibration Prediction

1 Introduction

Wind energy is one of the most developed renewable energy prospects. The world's wind power industry develops rapidly in recent years, as well the world's total wind turbines capacity reached 310 million kilowatts by the end of 2013. In recent years, Chinese wind turbines capacity increases rapidly, and becomes the largest one all over the world. However, China's wind power equipments are often operating in low efficiency, and the yearly average utilization time of a machine is only 1903

* Correspondence author (han1011@163.com)

 ISSN 2572-4975 (Print), 2572-4991 (Online)

hours comparing with the expected 2500 hours[1]. The main reason is due to many failures and poor reliability of the wind turbine machines.

The transmission chain system of wind turbine (except directly drive wind turbine) includes hub, shafts, bearings, and gearboxes. The gearbox is the major pathway of energy transfer and works under severe loading. The failure of the transmission system of wind turbine always causes the wind turbine shutdown at once.

Fourier spectral analysis has provided a general method for examining the global energy-frequency distributions, but has some inherent restrictions, for example, the system must be linear and the data must be strictly periodic or stationary. So how to identify or at least to distinguish the non-stationary properties of the signals is of major concerned. In recent years, some time-frequency processing methods for nonlinear and non-stationary signals have been proposed, such as wavelet analysis, Wigner-Ville distribution, etc [2-5].

Recently, a new method based on Hilbert-Huang transform (HHT) for analyzing non-stationary signals has been proposed[6], in which the expansion bases are adaptive for signals from nonlinear and non-stationary processes. Based on this method, any complicated signals can be decomposed into a finite and often small number of 'Intrinsic Mode Functions' (IMFs) that admit well-behaved Hilbert transforms. And with the Hilbert transform, the IMFs yield instantaneous frequencies as functions of time that give sharp identifications of embedded structures. The final presentation of the results is an energy-frequency-time distribution, designated as the Hilbert spectrum [7-9].

In this paper, vibration signals of the gearbox of wind turbines under different rated input loads are analyzed. From their time and frequency domain waveforms, they are not easily to be distinguished. In using HHT, we obtain effective distinctions between them. The results demonstrate that HHT is effective to identify the features of vibration signals of the gearbox of wind turbines under different rated input loads.

2 Basic algorithm procedure of HHT

HHT involves two aspects: empirical mode decomposition (EMD) and Hilbert spectral analysis (HAS)[6]. Firstly, a time-adaptive decomposing operation named EMD is applied to a signal, in which the signal are decomposed into a set of complete and almost orthogonal components named Intrinsic Mode Functions (IMFs). Secondly, with Hilbert transforming of those IMFs, a full energy-frequency-time distribution of the signal is obtained and designated as HAS [10- 11].

The IMFs, which are regarded as both the amplitude modulation and the frequency modulation, satisfy the following requirements: 1) the number of extremes and the number of zero crossings in the IMF must either be equal or different at most by one; and 2) at any point the mean value of the envelopes defined by the local maxima and local minima must be zero. The process to find the IMFs of a signal $x(t)$ comprises the following steps:

1) Find the positions and amplitudes of all local maxima and minima in the input signal $x(t)$. Then create an upper envelope by cubic spline interpolation of the local maxima, and a lower envelope by cubic spline interpolation of the local minima.

2) Calculate the mean of the upper and lower envelopes; this is defined as $m_1(t)$.

3) Subtract the envelope mean from the original input signal,

$$h_1(t) = x(t) - m_1(t) \tag{1}$$

4) Check whether $h_1(t)$ meets the requirements to be an IMF. If the sifting result $h_1(t)$ is an IMF, stop the process. Otherwise, treat $h_1(t)$ as the new signal data and iterate on $h_1(t)$ through the previous step 1) ~ 4). That is, to set

$$h_{11}(t) = h_1(t) - m_{11}(t) \tag{2}$$

Repeat this sifting procedure k times until $h_{1k}(t)$ is an IMF. This is designated as the first IMF, shown below

$$c_1(t) = h_{1k}(t) \tag{3}$$

5) Subtract $c_1(t)$ from the input signal and define the remainder, $r_1(t)$, which is the first residue as following,

$$r_1(t) = x(t) - c_1(t) \tag{4}$$

6) Since the residue $r_1(t)$ still contains information related to longer period components, it is treated as a new data stream and the above-described sifting process is repeated until the last IMF.

This procedure can be repeated n times to generate n residues, $r_n(t)$, and result in

$$r_2(t) = r_1(t) - c_2(t), \ldots, r_n(t) = r_{n-1}(t) - c_n(t) \tag{5}$$

The sifting process stops when either of two criteria are met: 1) the component $c_n(t)$, or the residue $r_n(t)$, becomes so small as to be considered inconsequential; or 2) the residue, $r_n(t)$, becomes a monotonic function from which an IMF can not be extracted. For example, the stopping condition for an IMF is

$$\sum_t \frac{[h_{k-1}(t) - h_k(t)]^2}{h_{k-1}^2(t)} < S \tag{6}$$

where $h_k(t)$ is the sifting result in the kth iteration, and S is typically set between 0.2 and 0.3. Besides, in order to achieve the last IMF, a simple way can be used. The last IMF could be obtained when the cubic spline fitting stops due to the number of local maxima or minima of the residue is less than 2.

Finally, we obtain

$$x(t) = \sum_{j=1}^{n} c_j(t) + r_n(t) \tag{7}$$

In other words, the original signal can now be represented as the sum of a set of IMFs plus a residue.

Now apply Hilbert transform to all IMFs,

$$H\left[c_j(t)\right] = \frac{1}{\pi} \int_{-\infty}^{\infty} \frac{c_j(\tau)}{t - \tau} \mathrm{d}\tau \tag{8}$$

 ISSN 2572-4975 (Print), 2572-4991 (Online)

After the Hilbert transform, $H\left[c_j(t)\right]$ and $c_j(t)$ form a complex signal. So, the envelope of every IMF, $c_j(t)$, is given by

$$a_j(t)=\sqrt{c_j^2(t)+(H[c_j(t)])^2} \tag{9}$$

The phase functions are

$$\Phi_j(t)=\arctan\frac{H[c_j(t)]}{c_j(t)} \tag{10}$$

And the instantaneous frequencies are obtained as

$$\omega_j(t)=\frac{\mathrm{d}\Phi_j(t)}{\mathrm{d}t} \tag{11}$$

Having obtained the components of IMFs, we will have no difficulty to apply Hilbert transform to each component of them. With the Hilbert transform of each IMF component, we can express the signal in the following form,

$$X(t)=\sum_{j=1}^{n}a_j(t)\exp(i\int\omega_j(t)dt) \tag{12}$$

Equation (12) also enables us to represent the amplitude and the instantaneous frequency as functions of time in a three-dimensional space, in which the amplitude can be contoured on the frequency-time plane. This frequency-time distribution of the amplitude is designated as the Hilbert amplitude spectrum, i.e. $H(\omega,t)$. With the Hilbert spectrum defined, we can also define the marginal spectrum, i.e. $h(\omega)$, as following

$$h(\omega)=\int_0^T H(\omega,t)dt \tag{13}$$

The marginal spectrum offers a measurement of the total amplitude (or energy) contribution.

3 Structure description and measuring method of wind turbine gearbox

The wind field tests on the 5MW wind power unit transmission chain are shown in Fig. 1. It is a ring gear driving planetary gear train, fixed axis gear train and a fixed parallel shaft gear set. The basic parameters and rated input power are shown in table 1. Speed ratio of the 1st stage is 4.333. Speed ratio of the 2nd stage is 3.609 and speed ratio of parallel shaft is 6.550, the total speed ratio is 102.426. The 1st stage has three planet gears.The on-site measurement of gearbox is shown in Fig. 2. The testing points are selected as shown in Fig. 3 in which the numbers '1' - '9' indicate the points of putting accelerators, and the letter 'F' refers to the reference point.

Table 1. Parameters and rated input load

rated input power	5730kW
rated input speed	11.9r/min
Transmission type	NW planetary + 1st stage parallel shaft
Total transmission ratio	102.426

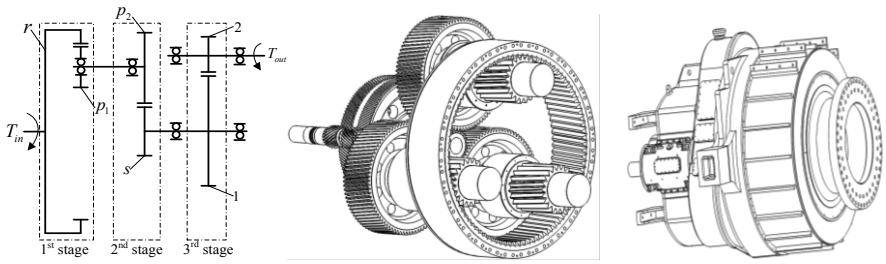

(a) Transmission principle (b) Gear system (c) 3D model

Fig. 1. Wind turbine gearbox driven by ring gear

Fig. 2. The on-site measurement of gearbox

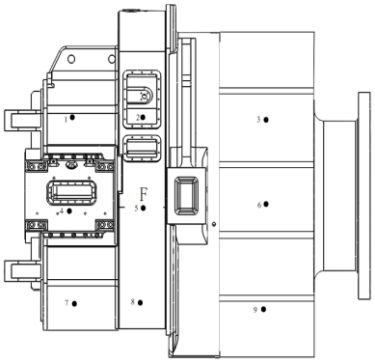

Fig. 3. The test points on the gearbox

4 Results

The vibration sensors are fixed as closely as possible to the measured objects and the rotating parts. The sampling frequency of vibration data is 10.24 kHz. Some of the measured vibrations at the measuring points of No.3 at case of 50% and 110% rated load are shown in Figure 4. Point 3 is on high speed shaft.

The vibration signals of point 3 are shown in Figure4, and their spectrum are shown in Figure 5 correspondingly. From Figure 4 and Figure 5, one cannot easily identify one from each other. The obtained spectrum of them in Figure 5 only show that they

ISSN 2572-4975 (Print), 2572-4991 (Online)

are both in limited frequency band distributions of 0-3000Hz with slightly different shapes.

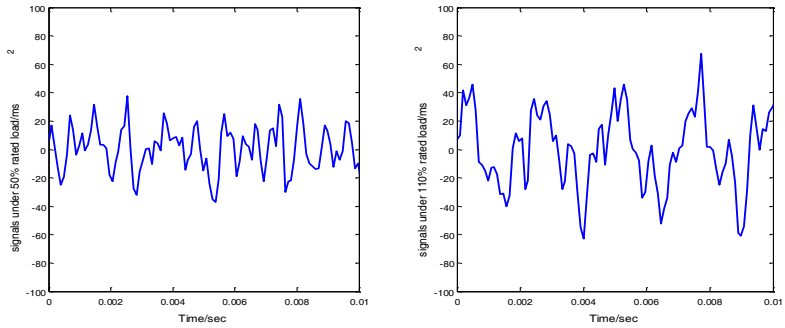

Fig. 4. The vibration responses picked at point 3 at case of 50% and 110% rated load

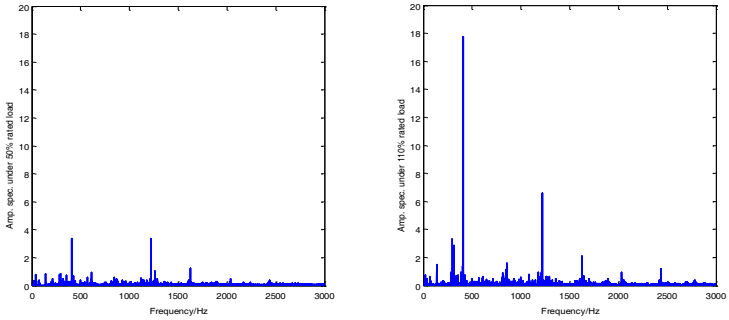

(a) 50% rated load (b) 110% rated load

Fig. 5. The spectrum of vibration signals of point 3 at case of 50% and 110% rated load

Now apply HHT for the two signals. The calculated IMFs and instantaneous frequencies (IFs) of point 3 are shown in Figure 6 and Figure 7.

From Figure 6 (a) and (b), we can see that there are ten IMF components for vibration signal of point 3 at case of 50% rated load, and ten IMF components for signal vibration signal of point 3 at case of 110% rated load separately. So we can say the signal at case of 50% and 110% rated load contain different frequency components which embody their different complexity in quantitative way. The first IMF of signals at case of 50% rated load, c1, appears as amplitude modulation, is also completely different from that in signals at case of 110% rated load. The second and third orders of the IMFs of signals at case of 50% rated load, i.e. c2 and c3, appear frequency modulations, while signals at case of 110% rated load is not. Correspondingly, IF of every IMF of signals at case of 50% and 110% rated load are shown in Figure 7 (a) and (b), which are physically meaningful, and the differences between signals at case of 50% and 110% rated load are clearer.

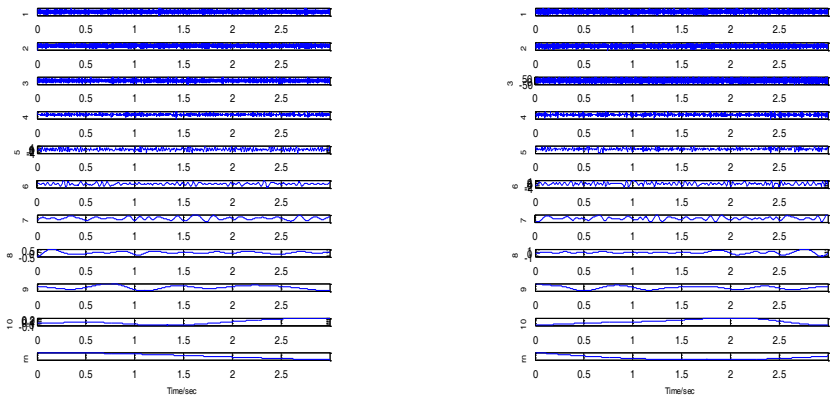

(a) 50% rated load (b) 50% rated load

Fig. 6. HHT analysis of vibration signals at point 3 at case of 50% and 110% rated load

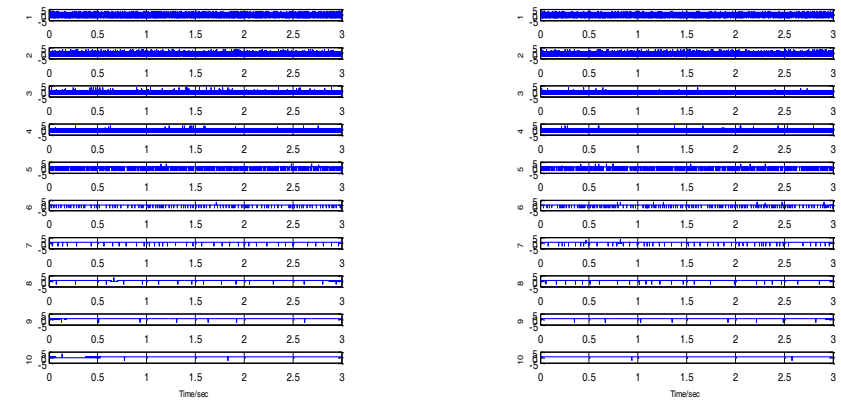

(a) Instantaneous frequencies at case of 50% (b) Instantaneous frequencies at case of 110%

Fig. 7 . Instantaneous frequencies of vibration signals at point 3 at case of 50% and 110% rated load

Furthermore, their Hilbert spectra and marginal spectra are also obtained according to the results of IMFs. They are shown in Figure 8 and Figure 9, respectively.

From the definition of Hilbert spectrum, we can know the Hilbert spectrum appears only in the skeleton (or line) form with emphasis on the frequency variations of each IMF. Because it gives more quantitative results, the skeleton presentation is more desirable. In Figure 8 (a) and (b), the Hilbert spectra of vibration signals under different rated input load are shown. We can distinguish easily the frequency variations of each IMF of vibration signals at point 3 under different rated input load

 ISSN 2572-4975 (Print), 2572-4991 (Online)

easily. Although the frequency variations of each IMF of vibration signals under different rated input load focus on within 50Hz, the vibration signals under 110% rated input load are more concentrated and marked, but the vibration signals under 50% rated input load are discrete relatively.

For the marginal spectra of vibration signals under different rated input load are shown in Figure 9, they offer the measurements of the total amplitude contributions from each frequency value. From Figure 9, we can find the values and their tendency of the total amplitude contributions of vibration signals under different rated input load are remarkable different. Vibration signals under 110% rated input load reaches to the maximum accumulation around 10Hz. We can distinguish the differences between them as well.

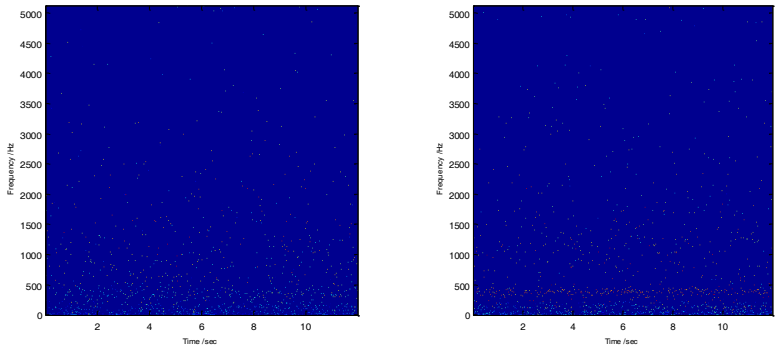

(a) 50% rated load (b) 110% rated load

Fig. 8. The Hilbert spectra of vibration signals at case of differnt rated load

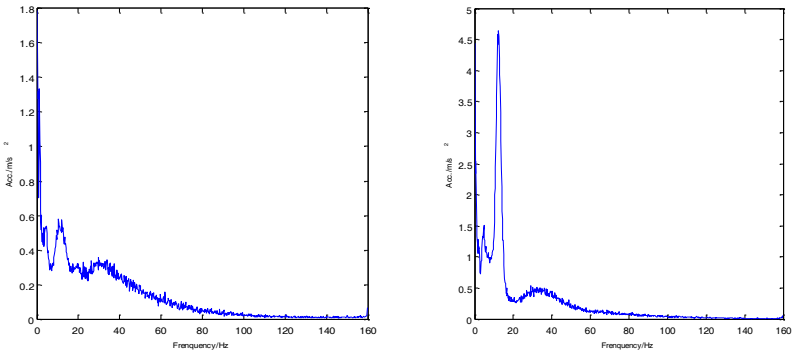

(a) 50% rated load (b) 110% rated load

Fig. 9. The marginal spectrum of vibration signals under differnt rated input load

5 Conclusion

Two different non-stationary signals are used as examples to be described and distinguished in the time-frequency analyses of HHT in the paper. The technique of HHT is proved to be effective on processing and distinguishing the differences of the vibration signals under differnt rated input load.

For the original signals given here, the obtained IMFs with HHT are easily distinguished from each others. The Hilbert spectra and the margin spectra are also different between them. These results demonstrate that the HHT can offer a more effective way for identifying the different features of vibration signals under differnt rated input load.

References

1. China State Electricity Regulatory Commission, ***Wind power safety supervision report***, 2012.
2. Parrish J C. , The Ranger Telerobotic Flight Experiment: A Teleservicing system for On-orbit Spacecraft, Telemanipulator and Telepresence Technologies III, ***In Proceedings of the SPIE***, Stein, M. R. ed., 177-185, (1996).
3. Zizeng Pei, ***The active vibration control of piezoelectric intelligent cantilever beam***, Shanxi, Master's thesis of Xi'an Electronic and Science University, 2011.
4. Lane J S, Dickerson S L., Contribution of passive damping to the control of flexible manipulators, ***Proceedings of the International Computers in Engineering Conference***, 1984,175-180,(1984).
5. Alberts T E, Dickerson S L, Book W J., On the transfer function modeling of flexible structures with distributed damping, ASME, 1986,3, 23-30, (1986).
6. Sakawa Y., Modeling and feedback control of flexible arm, ***Journal of Robotics System***, 2 (1985) 453 - 472.
7. Bailey T L, Hubbard J E., Distributed piezoelectric-polymer active vibration control of a cantilever beam, ***Journal of Guidance, Control and Dynamics***, 8(1985), 605-611.
8. Xingwei Guo, Research on filtering technology of accelerometer signal, ***Science and Technology Innovation Herald***, 22(2008)4.
9. Huang, N.E., Shen, Z., and Long, S. R., A new view of nonlinear water waves: the Hilbert Spectrum, ***Annu.Rev.Fluid Mech***, 31 (1999) 417–457.
10. Cheng, S.J., Yu, D.J., Yang,Y., The application of the energy operator demodulation approach based on EMD in machinery fault diagnosis, ***Mechanical Systems and Signal Processing***, 21(2007) 668-677.
11. Peng, Z. K., Chu, F. L., A comparison study of improved Hilbert–Huang transform and wavelet transform: Application to fault diagnosis for rolling bearing, ***Mechanical Systems and Signal Processing***, 19(2005) 974–988.

 ISSN 2572-4975 (Print), 2572-4991 (Online)